# Study of Coupling mechanism of optical and acoustic energy in the Time Resolved Pulsed Photoacoustic spectrum of I2 molecules at Different Temperature and Pressure.

F. Yehya[1] and A. K. Chaudhary[2]*

. [1]*Department of Physics, Faculty of Education &Sciences, Rada'a, Albaydha University, Albaydha Yemen*

*Advanced Centre of Research in High Energy Materials, University of Hyderabad, Hyderabad-500 046, India*

**E-mail:* [1]fahembajash@gmail.com & [2]anilphys@yahoo.com

DOI: https://doi.org/10.56807/buj.v3i2.138

***Abstract***

*The paper reports the time resolved pulsed photoacoustic study of I2 molecules using a single 532 nm, pulses of 7 ns duration at 10 Hz repetition rate obtained from Q- switched Nd: YAG laser. Frank -Condon principle based assignments confirms the presence of several numbers of ( v"- v') vibrational transitions covered by a single 532 + 2nm pulse profile. The strongest vibronic transition lines correspond to (32-0) and (31-0) transitions have the maximum intensities and part of equally separated bandwidth of the laser pulse. These strongest acoustic modes of I2 molecules are located at 4000 Hz and 14650 Hz, respectively. The separation of frequency between these two strongest modes is of the order of 10650 Hz. The experiment was repeated with different sized PA cell and found once again that two strongest acoustic modes of I2 molecules occur at 10.75 KHz and 21.45 KHz frequency range are separated by 10650 Hz only. For the first time, our experimental findings confirm that the frequency of the excited modes are controlled by cavity dimension whereas separation between the two strongest cavity modes are governed by the laser pulse profile. Moreover, the pressure and temperature based study demonstrates the exchange energy mechanism between the excited acoustic modes inside the PA cavity.*

*Keywords**: I2; Photoacoustic; modes; vibronic; pulsed laser.*

**Introduction:**

Iodine and bromine play very important role in gas phase photochemistry and heterogeneous reaction as aerosol. Their derivatives change the oxidation capacity of the troposphere and responsible for the depletion of Ozone layer. [1-2]

Ozone layer gets depleted by a number of free radical catalysts, such as hydroxyl radical (OH·), nitric oxide radical (NO·), atomic chlorine ion (Cl·), atomic bromine (Br·) and iodine ions.

The Bromine and Iodine atoms/ ions coming from sea beds in form of BrO or IO destroy the ozone molecules through a variety of catalytic cycles. For example, a bromine atom reacts with an ozone molecule in the troposphere and forms BrO and release a normal oxygen molecule.

$$X + O_3 \rightarrow XO + O_2 \quad (X = Br, I) \qquad (1)$$

Iodine atoms can also react with ozone to produce the iodine monoxide (IO) radical [3-5]:

$$I + O_3 \rightarrow IO + O_2 \qquad (2)$$

The most important reaction of IO is with $HO_2$ to produce hypoiodous acid (HOI) which works as a temporary iodine reservoir.

$$IO + HO_2 \rightarrow HOI + O_2 \qquad (3)$$

Due to the advancement of laser technology along with significant progress in the designing and sensitivity of microphones and data acquisition system the present form of photoacoustic spectroscopy becomes one of the most efficient and versatile tool to study the non-radiative relaxation transition in solid, liquid and gas samples [6-14].

Fig-1 shows that, $I_2$ has different repulsive curves which are expected to touch or cross the $B^3\pi(O_u^+)$ state [15-17]. Fluorescence experiments of Kruzel et al indicated the existence of vibrational and rotational relaxations in the B state of $I_2$ and it is expected that similar type of relaxations occurs in the other halogens too [18]. Venkateswarlu et al have studied the photoacoustic spectra for $I_2$ between the 15150-17520 $cm^{-1}$ and 16040-17280 $cm^{-1}$ range, respectively [19]. They have also recorded the $I_2$ spectrum in the range of 18900-20000$cm^{-1}$. Their analyses show that the photo acoustic spectrum of $I_2$ is due to the transition between $X^1\Sigma_g^0 \rightarrow B^3\pi(O_u^+)$ level.

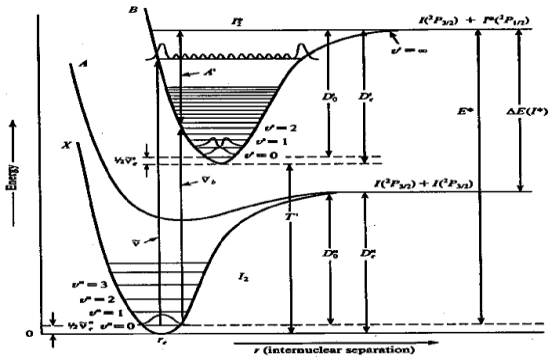


Fig-1: Partial Potential Diagram of $I_2$

The extensive work on vibrational analysis of the optical absorption spectrum of iodine molecules in form of atlas has been reported by Luc et al [20,21].Narayanan et al, have reported that the photo acoustic signal generated by $I_2$ molecules using 532 nm for $I_2$ is due to transition between $X^1\Sigma_g^0 \rightarrow B^3\pi(O_u^+)$ $states$. This is mainly due to (32,0),(33,0)and (34,0) relaxation vibrational states of $I_2$ [22].

In addition, Venkateswarlu has also shown the presence of partially resolved rotational structure in the PA spectrum of $I_2$ molecules in the 16797-16895$cm^{-1}$ region. The $I_2$ atlas confirm that these rotational lines belong to (14, 2) and (21, 1) bands [23].

Mariner et al reported the Doppler-free photoacoustic spectroscopy on the P(193) line of the (11-0) band of $I_2$ by resolving the hyperfine structure[24]. These studies confirm the role of photoacoustic spectroscopy technique for recording of non-radiative relaxation transitions of $I_2$ molecules.

The present study discusses the coupling mechanism of optical and acoustic energy in $I_2$ molecules. To the best of our knowledge, this is the first demonstration of twelve numbers of time resolved PA spectrum of I2 molecule produced by single nanosecond pulse of 532 nm . The Franck-Condon based theoretical calculations of vibronic transitions are verified experimentally. The study also highlights some of the interesting features of different types of acoustic modes with respect to pressure and temperature. We have experimentally demonstrated that some of the simultaneously excited acoustic modes show different decay behavior inside the resonant cavity. In addition, the separation between two strong excited finger print acoustic modes is independent on the dimension of the PA Cell.

## 1. Experimental set-up :

We have used λ=532 nm wavelength i.e. second harmonic of Q-switched Nd: YAG laser (Model Spit, Germany) to excite the $I_2$ vapour in the PA Cells. These cells are made of stainless steel and designed and fabricated in the laboratory itself. Their internal diameters are 2.8cm and 1.5cm with average length of 16 and 26 cm respectively [25]. The PA signal is detected by a pre-polarized microphones having responsivity 50mV/Pa (BSWA, China made). The microphones are placed in the center of the cells. The output signal of the microphone is fed to the preamplifier which is coupled to the 200 MHz Oscilloscope (Tektronix made in U.S.A.). The USB /GPIB interfacing was used for data acquisition through Boxcar integrator (Stanford Instruments Inc., USA made). The data analysis is done using Lab view software .

## 2. Results and Discussion:

The obtained results are divided into following four subsections (4.1- 4.4):

### 2.1 Allowed vibronic transitions of Iodine around 532nm:

We have calculated the vibronic transition of $I_2$ molecules at 532nm wavelength using the following equation:

$$IOA = Qv',v''exp(-DEv''/kT) \ldots\ldots\ldots\ldots (5)$$

where $Q\ v',v''$ is the Franck-Condon(F. C) factor for the vibronical bands $(v',v'')$, – D$Ev''$ refers to the vibronical energy in the ground electronic state with respect to $v''$ = 0, κ *is* the Boltzmann constant and $T$ is the absolute temperature of the photoacoustic cell.

Table–1 shows some selected transitions of vibronic levels of $I_2$ molecules exited by 532nm wavelength of pulsed Nd: YAG laser.

Table-1: Assignments and Absorption intensity of allowed vibronical levels of $I_2$ at 532 ±2nm

| *NO.* | *Band freq.($cm^{-1}$)* | *F-C factor* | *Wavelength (nm)* | *Assignments (v",v')* | *Lines Absorption Intensity* |
|---|---|---|---|---|---|
| **1** | **18834** | **0.03125** | **530.95** | **(32-0)** | **3.125** |
| **2** | **18809** | **4.23E-05** | **531.66** | **(35-1)** | **1.52** |
| **3** | **18789** | **0.002826** | **532.23** | **(56-5)** | **0.0018** |
| **4** | **18767** | **0.003165** | **532.84** | **(55-5)** | **0.002** |
| **5** | **18767** | **0.03178** | **532.85** | **(31-0)** | **3.178** |
| **6** | **18767** | **0.01217** | **532.85** | **(38-2)** | **0.1591** |
| **7** | **18753** | **0.003617** | **533.24** | **(42-3)** | **0.0172** |
| **8** | **18748** | **0.00037** | **533.39** | **(34-1)** | **1.3301** |
| **9** | **18746** | **0.000735** | **533.46** | **(47-4)** | **0.0013** |
| **10** | **18780** | **0.000412** | **533.47** | **(48-4)** | **0.0007** |
| **11** | **18744** | **0.00352** | **533.49** | **(54-5)** | **0.0023** |
| **12** | **18720** | **0.003886** | **534.2** | **(53-5)** | **0.0025** |

There are 12 numbers of vibronic levels (*v'-v"*) transition of different intensities covered by a pulse of 532 nm. The corresponding assignment of relative optical absorption intensity is shown in the fifth column of table-1. Fig-2 shows the calculated values of absorption intensity distribution of these vibronical levels. One can see that the strongest vibronic transitions are not located at the peak value of 532nm. However, the strongest vibronic transition lines due to transition between (32-0) and (31-0) levels have maximum intensity and equally separated from bandwidth of 532nm of the laser pulse. It is also to be noted that the distribution of actual signal depends directly on the energy distribution of laser pulse profile.

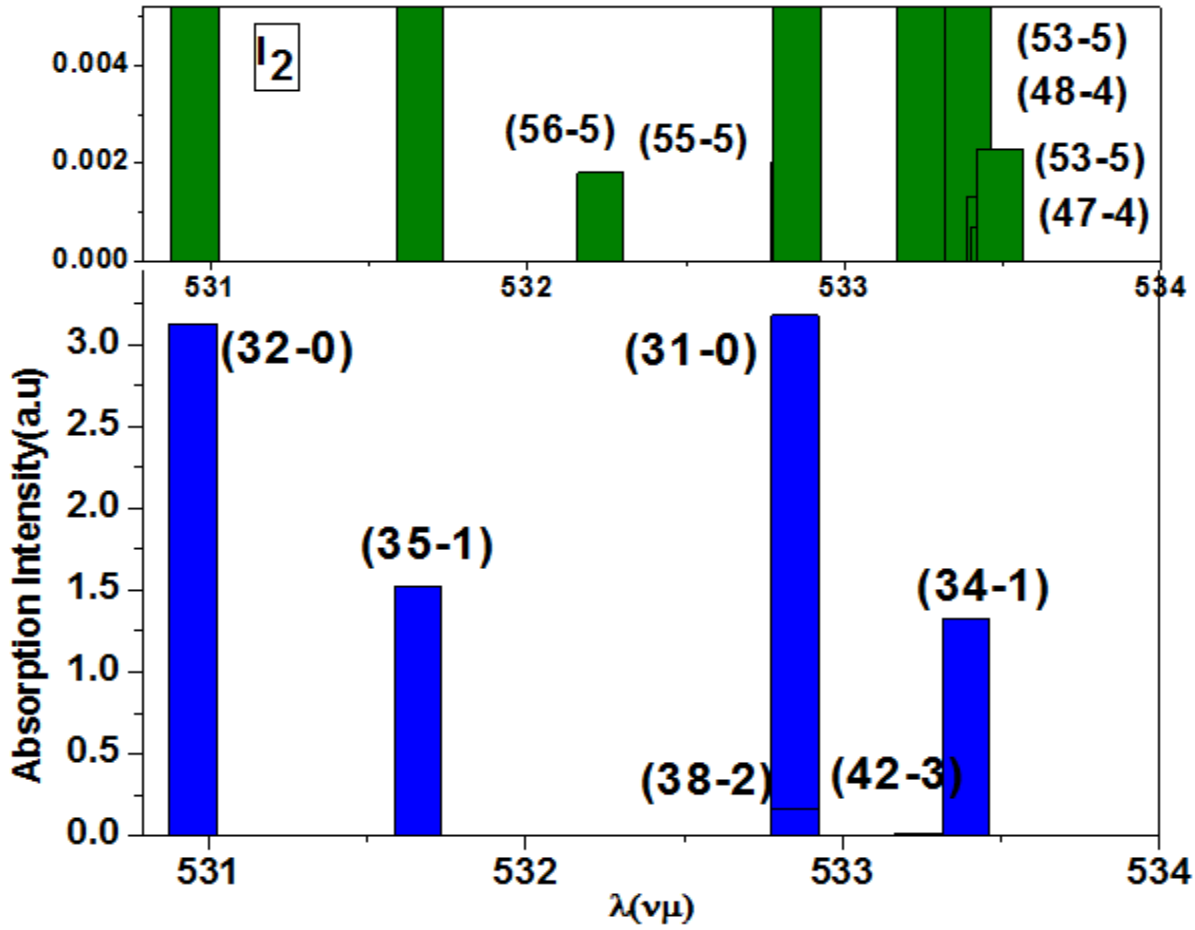


Fig-2: Absorption intensity of vibronic modes around 532nm (upper part is the amplify of the smallest transitions)

## 2.2 PA spectrum of Iodine in PA Cells

The PA spectrum of $I_2$ at 220 Torr pressure and at 25 mJ input energy of the laser are displayed in Fig-3. The inset shows the time-domain PA signal, while the main frame shows the frequency domain spectrum of $I_2$ obtained by a fast Fourier transform (FFT). The PA spectrum of $I_2$ shows the presence of multimode excited lines of $I_2$ molecules due to multiple transitions between B-X bands. The strongest acoustic modes of $I_2$ molecules are located at 4000 and 14650 Hz. The separation of frequency between these two strongest modes is 10650 Hz.

Here, the coupling between optical energy distribution and acoustic energy distribution can be understood as follows. The strongest vibronic modes of $I_2$ molecules have equally been distributed around 532nm. These acoustic modes correspond to the absorption of the optical energy are located at 4.0 kHz and 14.65 kHz, respectively. Moreover, in both cases there is no formation of clusters due to unavailability of closed vibronic modes at 532 nm. Also both figures have several small modes located in different range of acoustic frequencies and laser wavelengths. However, the strongest vibronic transitions at (32-0) and (31-0) are located at two ends of FWHM of 532 nm pulse which corresponds to equal absorption of laser pulse energy.

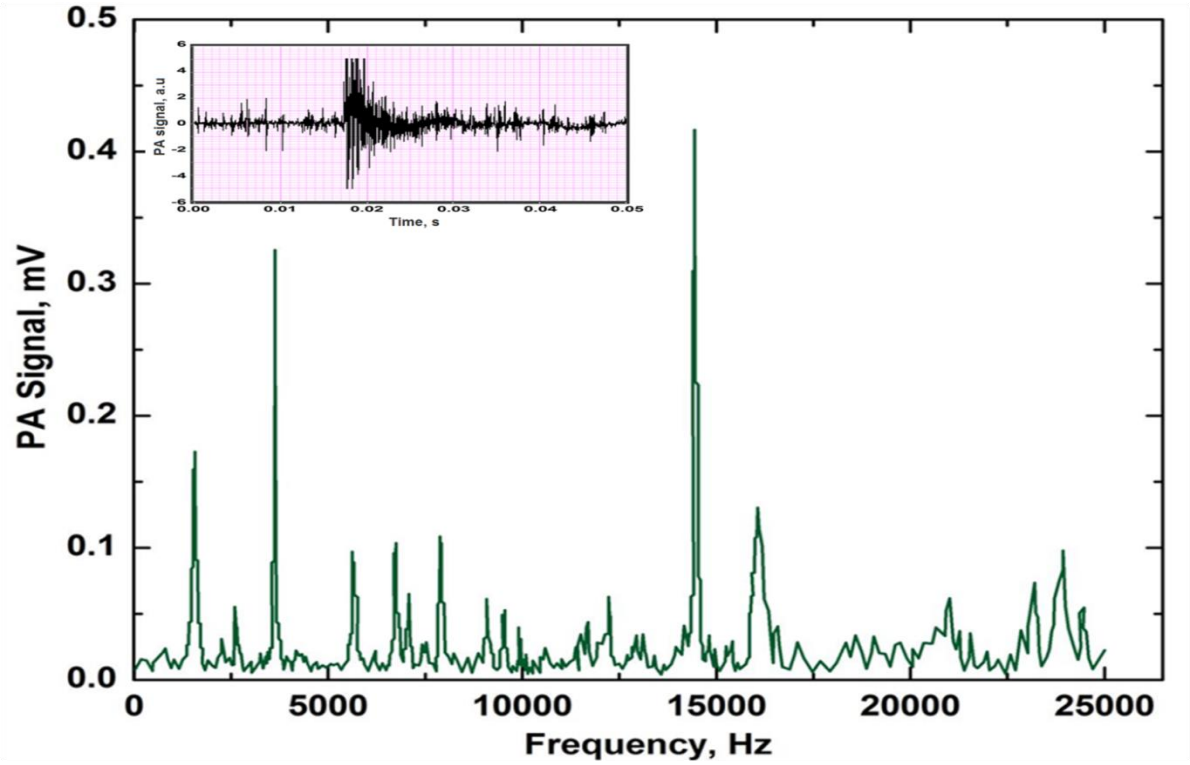


Fig-3: PA spectral of $I_2$ in PA cell (L=16cm & R=1.4cm)

Fig-4 shows the PA spectrum of $I_2$ vapour in PA cell (L=65mm, R=7.5mm). Here also the PA spectrum shows the similar type of spectrum profile. Once again we have identified two strongest modes at 10.75 and 21.45 kHz, respectively. The separation of frequency between these two modes is around 10700 Hz which is almost similar to the previous cell value. In addition, other small excited modes occupy different range of frequencies.

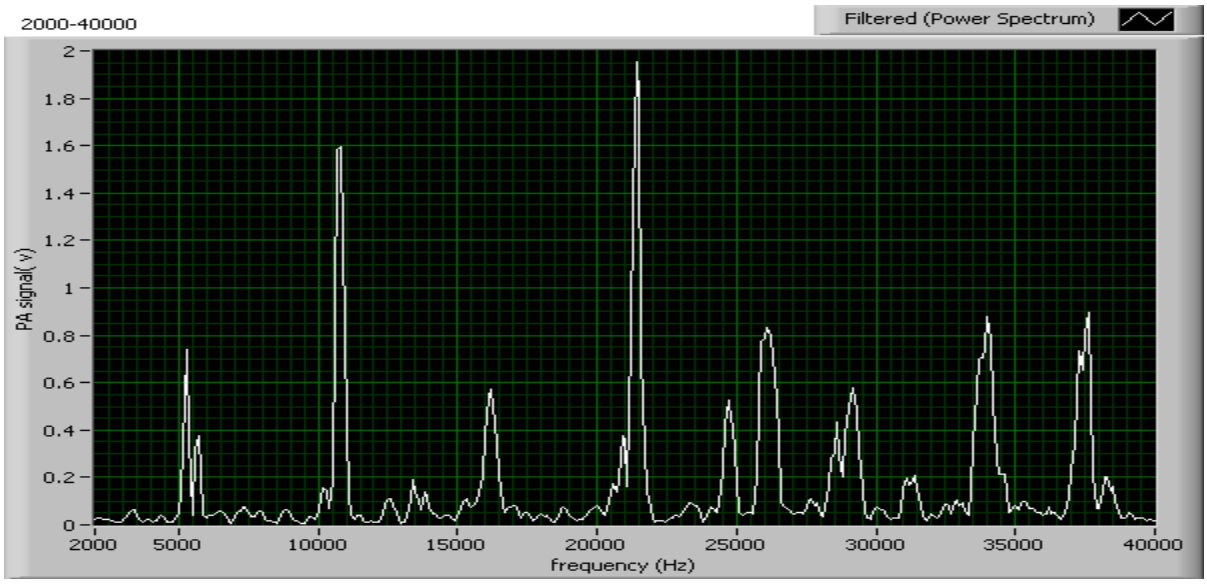


Fig-4: PA spectrum of $I_2$ at 220 Torr (L=65mm & R=7.5mm)

### 2.3 Pressure dependent behaviour of Iodine ($I_2$) vapour in PA cell (L=16cm, R=1.4cm):

The presence of multiple lines in the time domain spectrum of $I_2$ molecules is due to strong absorption of this gas in the visible range. Therefore, it is quite interesting to study the pressure dependent behaviour of different excited modes of $I_2$. This helps us to understand their dynamics at different pressures. Fig-5 shows an interesting rise and decay behavior of two different excited modes of the $I_2$ molecules as a function of pressure. In case of 4 kHz mode the strength of PA signal start to decrease when pressure exceeds more than 350 Torr while acoustic mode at 14.6 kHz shows the rapid growth upto 300 torr pressure . The process of rise of 4 kHz mode and fall of 14.6 kHz modes occurs simultaneously which is only due to the exchange of energy among these modes .

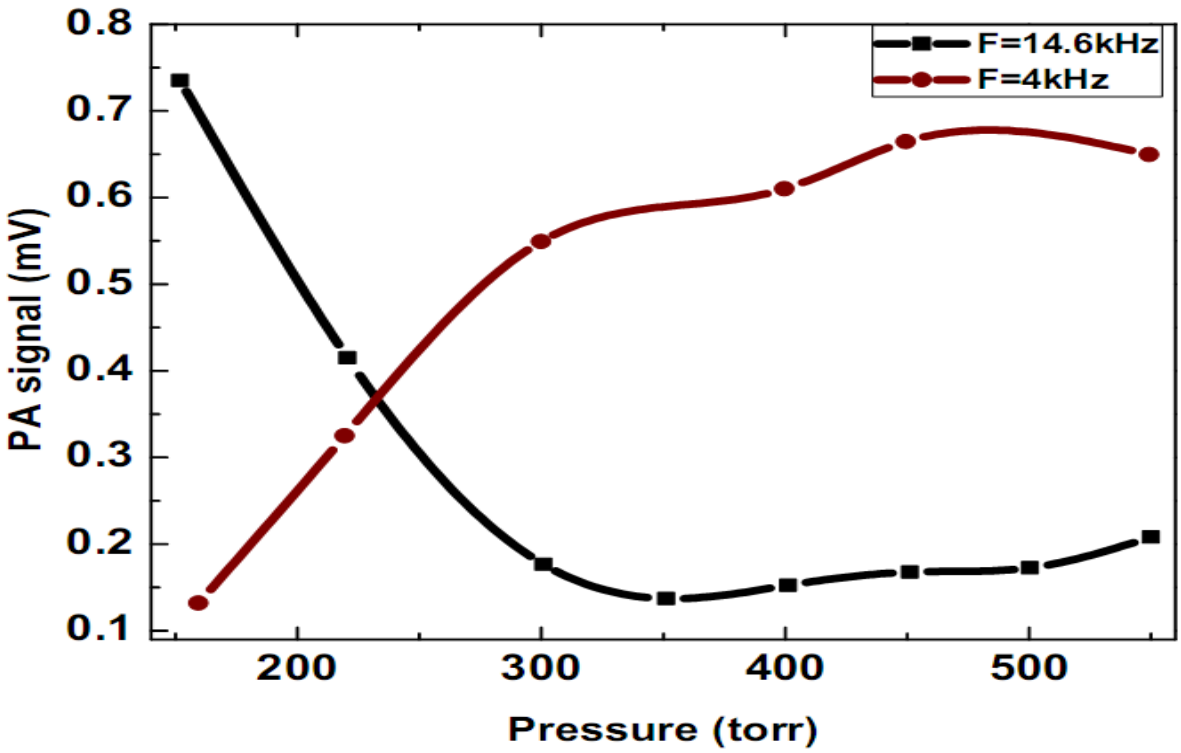


Fig-5: The pressure dependent behavior of PA modes at 4 kHz and 14.6 kHz .

### 2.4 Temperature dependent behavior of Iodine ($I_2$) vapor:

Fig-6 (a) and (b) show the behavior of three different excited modes of the $I_2$ molecules with respect to different temperatures. It is very much interesting to see that the strength of PA signals at 10.9 KHz and 20.45 kHz show some gain while other excited modes show decaying behavior.

Fig-7(a) represents the temperature behavior at mode at 10.9 kHz frequency. The strength of PA signal increased with respect to temperature while fig-7(b) shows the behavior of the resonance mode at 20.45 kHz. The strength of this mode starts increasing around 130 $^0$C

.

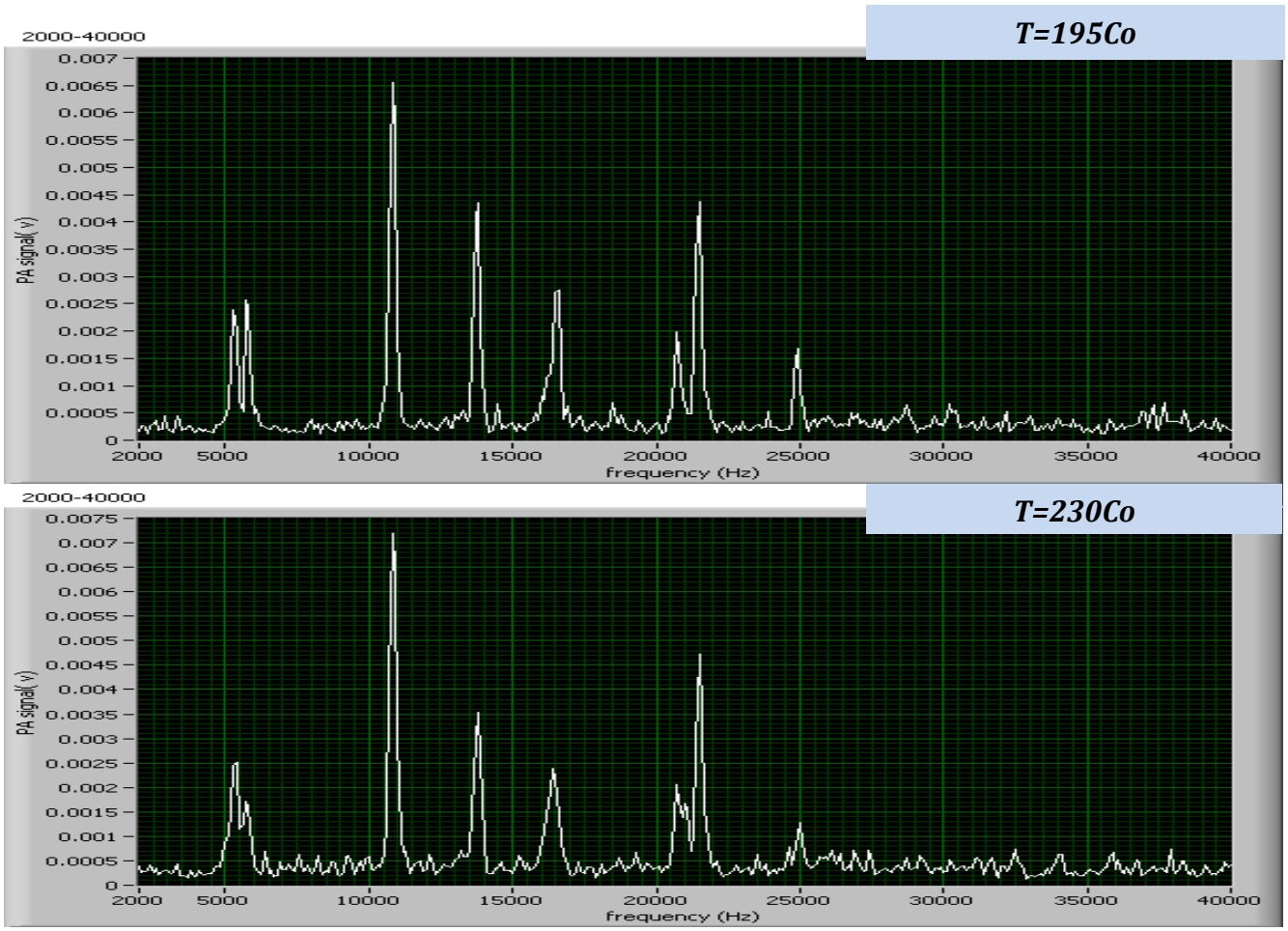


Fig- 6: FFT spectrum of PA signal at different temperature

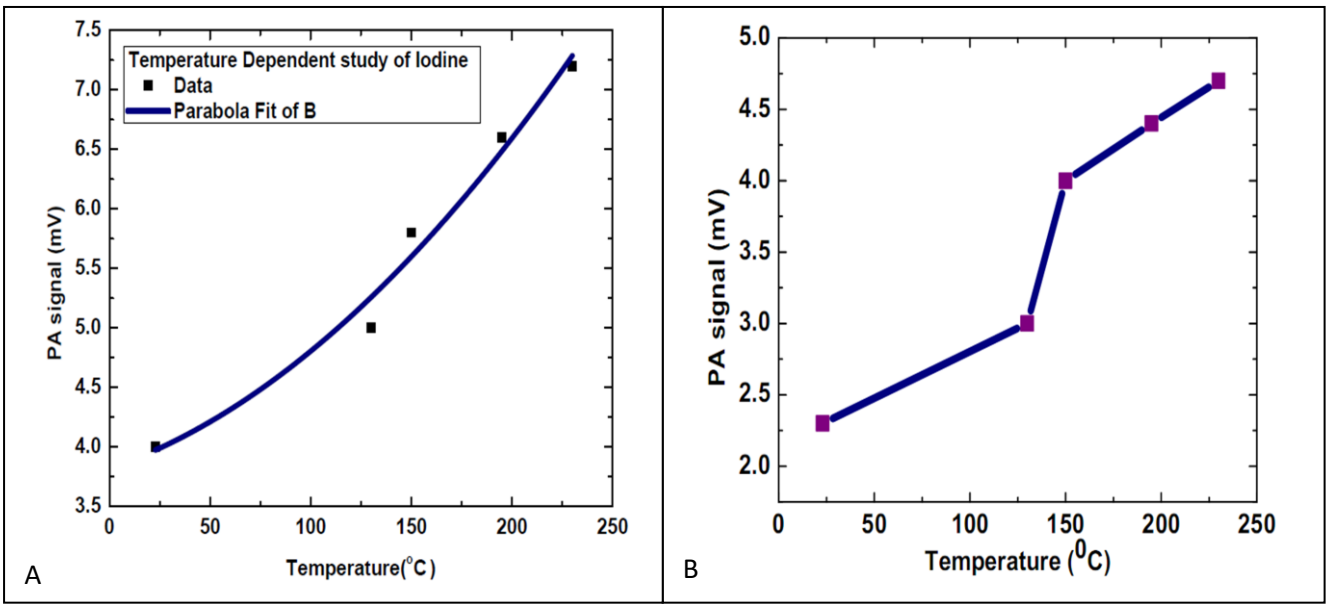


Fig- 7: Behaviour of a) 10.9 kHz and b) 20.45kHz at different temperatures.

## 3. Conclusions:

We have theoretically calculated the different types of new acoustic modes in two different types of PA cells and experimentally verified for $I_2$ molecules using a single pulse of 532 nm wavelength. Frank -Condon principle based assignments confirm the presence of several numbers of ( ν”- ν’) vibronical transitions covered by a single 532 $\pm$ 2nm pulse profile. With the help of two different sized PA cells we have successfully demonstrated the position of strongest acoustic modes are governed by the PA cell dimension while separation of the modes is controlled by laser pulse width. On one side, the pressure studies also confirm the exchange of energy between the two strongly excited modes on other side temperature based study shows that strong mode tendency of growth while other satellite modes show the tendency of decay.

6. **References :**


[1] Carpenter, L. J. Jones, C. E. Dunk, R. M. Hornsby, K. E. Woeltjen, J. , (2009) , *Atmos. Chem. Phys.* 9 1805

[2] Hossaini, R. Chipperfield, W. Feng, T. J. et al. (2012) , *Atmos. Chem. Phys*. 12 371

[3] DeMore, W. B. Sander, S. P. ,, (1997), *(JPL Publication*, 97-4

[4] Huie, R. E. Laszlo, B. and Kurylo, M. J. “*The Atmospheric Chemistry of Iodine Monoxide*” (HOlWC.95, 311-322.)

[5] Voget, R. Sander, R. Glasow, R. V. Crutzen, P. J. *J*,. (1999) , *Atmospheric. Chem*. 32 375

[6] Sigrist, W.M., ,(1994),.*Air Monitoring by Spectroscopic Techniques*, (John Wiley and Sons, New York,

[7] Karbach, A. Hess. P. *J*., (1986), *Chem. Phys*. 84 2945

[8] Morse, P. M. ,(1948) ,“*Vibronic and Sound, Chap. 8* McGraw–Hill, New York,.

[9] Boz´oki, Z. et al. ,(2002), *Appl. Spectrosc*. 56(6) 715

[10] Guo, R. Chen, N-l Lai, E. P. C,(1988),. *Analyst.* 113 595

[11] Slater, J. C. , (1960), “Quantum theory of atomic structure” (McGraw-Hill vol. I)

[12] Kopp, C. and Niessner, R., (1998), *Analyst.* 123 547

[13] Weast, G. A. Barrett, J. J. Siebert, D. R. Reddy, K. V. *Rev.*, (1983), *Sci. Instrum*. 54 797

[14] Thony, A. Sigrist, M. W. ,(1995), *Infrared Phys. Technol*. 36(2) 585

[15] Mulliken, R. S , (1934)., *Phys. Rev*. 46 549

[16] Mulliken, R. S., (1934) , *Chem. Phys*. 55 549

[17] Asundi, R. K., (1947) , Venkateswarlu, P. *Indian. J. Phys*. 21 101

[18] Kruzel, R. B. Steinfeld, J. I. . (1971) ,Holtzenbuhler, D. A. Leroi, G. E. *J. Chem. Phys*. 554822

[19] Venkateswarlu, P. Kumer, D. McGlynn, S. P. proc. symp. on lasers and applications(eds) H D Bist and J. S. Goela (*New Delhi: Tata McGraw-Hill*)

[20] Gertenkorn, S. Luc, P. ,,( 1978) ,(*CNRS*, Paris

[21] Luc, P. *J. Mol. Spectrosc*. 40 (1980)41

[22] Narayanan, K. Thakur, S. N ,(1992)., *Appl. Opt.* 31 4987

[23] Venkateswarlu, P. Chakrapani, G. George, M. C. (1987) ,Rao, Y. V. and Okafor, C. *Pramana-J. Phy.* 29 261

[24] Marinero, E. E. Stuke, M. *Opt.*, (1979), *Commun*. 30 349.

[25] Yehya, F. Chaudhary, A. K ,(2013)., *Spectrochemica. Acta. A.* 115 544.